Reactive Collisions of $C_6H_6^{\bullet+}$ and $C_6D_6^{\bullet+}$ at Self-Assembled Monolayer Films Prepared on Gold from *n*-Alkanethiols and a Fluorinated Alkanethiol: The Influence of Chain Length on the Reactivity of the Films and the Neutralization of the Projectile

Árpád Somogyi,[†] Thomas E. Kane, Jian-Mei Ding, and Vicki H. Wysocki*

Contribution from the Department of Chemistry, Virginia Commonwealth University, Richmond, Virginia 23284-2006

Received October 22, 1992

Abstract: Low-energy ion-surface collisions were used to probe the reactivity, electron barrier properties, and relative degree of order of self-assembled monolayer films after transfer of the films from solution to vacuum (10^{-7} Torr). Mass-selected polyatomic projectiles (ionized benzene, benzene-d_6, and fluorobenzene) collided with self-assembled monolayer films at collision energies in the range of 20–70 eV, and the resulting ions were mass-analyzed and detected. The surfaces were prepared by the spontaneous assembly of *n*-alkanethiols ($CH_3(CH_2)_nSH$, $n = 3, 11, 17$), perdeuterioeicosanethiol ($CD_3(CD_2)_{19}SH$), and 2-(perfluorooctyl)ethanethiol ($CF_3(CF_2)_7CH_2CH_2SH$) on both gold foil and vapor-deposited gold. Chemical reactions between the benzene molecular ion and the monolayer films (e.g., H, CH_3, D, CD_3, F, and CF_3 additions) are evident from deuterium labeling results. Ion-surface collision spectra for ionized benzene are sensitive to (i) the chemical composition of the monolayer, (ii) the chain length of the alkanethiol used to prepare the film, (iii) the preparation of the gold surface prior to reaction (mechanically polished gold foil vs vapor-deposited gold vs plasma-cleaned vapor-deposited gold), and (iv) the exposure time between the alkanethiol solution and the gold. For comparison with our experimental results, *ab initio* calculations have also been carried out to predict the energetics of the loss of H and H_2 from selected ion-surface reaction adducts (H, F, and CH_3 addition products). Experimental data not directly available from the tandem mass spectra (i.e., total ion signals and surface currents) are used to characterize the relative degree of neutralization of the projectiles at the films. The data suggest that the relative electron barrier properties of the films in vacuum mimic those reported for electrochemistry experiments in solution. The mass spectra and the current measurements indicate that the relative degree of order of the monolayers is retained upon transfer of the films from solution to vacuum.

Introduction

Low-energy collisions of mass-selected polyatomic ions with a surface promote extensive, structurally characteristic fragmentation of the selected ion by conversion of a portion of the kinetic energy of the projectile ion into ion internal energy.[1-19] For systems investigated to date, 8–60% conversion has been reported.[1,2,7,9,14-16,19] Attractive features of this surface-induced dissociation (SID) technique are that the average internal (vibrational) energies deposited can be varied by changing the kinetic energy of the projectile ion and that high average internal

energies are deposited in a relatively narrow internal energy distribution.[1,9,16] Other processes, including ion-surface reactions, chemical sputtering, and neutralization of the projectile, may also occur upon ion-surface collisions. The relative contributions of these competitive processes depend on both the nature of the projectile ion and the nature of the surface. The majority of the ions appearing in the mass spectra originate, however, from surface-induced dissociation.

Recently, self-assembled monolayer films were shown to be effective surfaces for ion-surface collisions.[17-19] These modified surfaces are prepared in solution by the spontaneous assembly of 1-alkanethiols (or their derivatives) onto gold[20-32] or silver.[33,34] This forms highly ordered, covalently bound monolayer films

* Author to whom correspondence should be addressed.
† On leave from Central Research Institute for Chemistry of the Hungarian Academy of Sciences, P.O. Box 17, H-1525 Budapest, Hungary.
(1) Cooks, R. G.; Ast, T.; Mabud, Md. A. *Int. J. Mass Spectrom. Ion Processes* **1990,** *100,* 209.
(2) Bier, M. E.; Schwartz, J. C.; Schey, K. L.; Cooks, R. G. *Int. J. Mass Spectrom. Ion Processes* **1990,** *103,* 1.
(3) Schey, K. L.; Cooks, R. G.; Kraft, A.; Grix, R.; Wollnik, H. *Int. J. Mass Spectrom. Ion Processes* **1989,** *94,* 1.
(4) Ast, T.; Mabud, Md. A.; Cooks, R. G. *Int. J. Mass Spectrom. Ion Processes* **1988,** *82,* 131.
(5) Hayward, M. J.; Mabud, Md. A.; Cooks, R. G. *J. Am. Chem. Soc.* **1988,** *110,* 1343.
(6) Vincenti, M.; Cooks, R. G. *Org. Mass Spectrom.* **1988,** *23,* 317.
(7) Bier, M. E.; Amy, J. W.; Cooks, R. G.; Syka, J. E. P.; Ceja, P.; Stafford, G. *Int. J. Mass Spectrom. Ion Processes* **1987,** *77,* 31.
(8) Mabud, Md. A.; DeKrey, M. J.; Cooks, R. G.; Ast, T. *Int. J. Mass Spectrom. Ion Processes* **1986,** *69,* 277.
(9) DeKrey, M. J.; Kenttämaa, H. I.; Wysocki, V. H.; Cooks, R. G. *Org. Mass Spectrom.* **1986,** *21,* 193.
(10) Mabud, Md. A.; DeKrey, M. J.; Cooks, R. G. *Int. J. Mass Spectrom. Ion Processes* **1985,** *67,* 285.
(11) (a) Ijames, C. F.; Wilkins, C. L. *Anal. Chem.* **1990,** *62,* 1295. (b) Williams, E. R.; Henry, K. D.; McLafferty, F. W.; Shabanowitz, J.; Hunt, D. F. *J. Am. Soc. Mass Spectrom.* **1990,** *1,* 413.

(12) Aberth, W. *Anal. Chem.* **1990,** *62,* 609.
(13) Cole, R. B.; LeMeillour, S.; Tabet, J. C. *Anal. Chem.* **1992,** *64,* 365.
(14) Williams, E. R.; Jones, G. C., Jr.; Fang, L.; Zare, R. N.; Garrison, B. J.; Brenner, D. W. *J. Am. Chem. Soc.* **1992,** *114,* 3207.
(15) Beck, R. D.; St. John, P.; Alvarez, M. M.; Diederich, F.; Whetten, R. L. *J. Phys. Chem.* **1991,** *95,* 8402.
(16) Wysocki, V. H.; Ding, J.-M.; Jones, J. L.; Callahan, J. H.; King, F. L. *J. Am. Soc. Mass Spectrom.* **1992,** *3,* 27.
(17) Winger, B. E.; Julian, R. K., Jr.; Cooks, R. G.; Chidsey, C. E. D. *J. Am. Chem. Soc.* **1991,** *113,* 8967.
(18) (a) Wysocki, V. H.; Jones, J. L.; Ding, J.-M. *J. Am. Chem. Soc.* **1991,** *113,* 8969. (b) Somogyi, Á.; Kane, T. E.; Wysocki, V. H. *Org. Mass Spectrom.* **1993,** *28,* 283. (c) McCormack, A. L.; Somogyi, Á.; Dongré, A. R.; Wysocki, V. H. *Anal. Chem.,* submitted for publication.
(19) Morris, M.; Riederer, D. E., Jr.; Winger, B. E.; Cooks, R. G.; Ast, T.; Chidsey, C. E. D. *Int. J. Mass Spectrom. Ion Processes* **1992,** *122,* 181.
(20) Porter, M. D.; Bright, T. B.; Allara, D. L.; Chidsey, C. E. D. *J. Am. Chem. Soc.* **1987,** *109,* 3559.
(21) Strong, L.; Whitesides, G. M. *Langmuir* **1988,** *4,* 546.
(22) Bain, C. D.; Troughton, E. B.; Tao, Y.-T.; Evall, J.; Whitesides, G. M.; Nuzzo, R. G. *J. Am. Chem. Soc.* **1989,** *111,* 321.

that can be removed from solution and inserted into the vacuum chamber of a mass spectrometer. Self-assembled monolayer films[20-38] are stable, easy to prepare, and useful for the electrochemical properties[26-32] they impart to electrode surfaces. The films have been characterized by a wide variety of techniques,[20-34] such as simple wetting tests,[23,24,34] atomic force microscopy,[25] and secondary ion[27a] and laser desorption[27b] mass spectrometry. It has been shown that the polymethylene chains of the alkanethiolates[20,22] on gold exist in a crystalline-like environment, with the chains oriented trans zig-zag and fully extended with a chain tilt of approximately 30° relative to the surface normal.

For our investigation, monolayer films were prepared from (i) *n*-alkanethiols of different chain lengths ($CH_3(CH_2)_nSH$, $n = 3$, 11, 17), (ii) perdeuterioeicosanethiol ($CD_3(CD_2)_{19}SH$), and (iii) 2-(perfluorooctyl)ethanethiol ($CF_3(CF_2)_7CH_2CH_2SH$) on both gold foil and vapor-deposited gold. We discuss here the spectra that result when ionized benzene, ionized benzene-d_6, and ionized fluorobenzene collide with these self-assembled monolayer films at low kinetic energies (30–70 eV). The major focus of this article is not the dissociation of the selected ions, but rather ion-surface reactions and neutralization of the projectile.

Benzene was chosen to probe the reactivity of self-assembled monolayer films for several reasons. It is a relatively small and simple molecule; this limits the number of fragment ions that can compete with ion-surface reactions. A large body of literature exists on both (i) the unimolecular reactions of benzene, i.e., its dissociation patterns upon activation by photons or gas-phase collisions,[39] and (ii) the bimolecular reactions of benzene.[40,41] In addition, previous reports indicate that a methyl addition reaction, with subsequent H_2 loss, occurs between benzene radical ions and adventitious hydrocarbons adsorbed on metal surfaces.[1,4,5] When collisions between benzene and stainless steel were investigated in our laboratory, we detected not only the methyl addition reaction but also additions of alkyl groups larger than methyl. Corresponding reactions (e.g., addition of C_nH_m, $n > 1$) have been reported for larger aromatic hydrocarbons such as naphthalene, phenanthrene, and pyrene.[1-3,14,15]

In the work reported here, a labeled (perdeuterated) alkanethiolate film[17] is used to distinguish between reaction with the self-assembled monolayer film vs reaction with adventitious

hydrocarbons in the system. It is expected that the amount of physisorbed adventitious hydrocarbon present at the surface will be substantially decreased on the low free energy, self-assembled monolayer films as compared with that on metal surfaces. Labeled and unlabeled films and labeled and unlabeled benzene are also used to further explore the mechanism of the proposed reactions. In addition, the influence of the chain length of the alkanethiolate films on these reactions is explored, because literature reports show that the crystallinity of the surface varies with chain length.[20,22] Reactions at the fluorinated surface (F and CF_3 addition) are investigated for comparison with reactions at the alkanethiolate surfaces. In contrast with results obtained on alkanethiolate surfaces, no surface reactions were detected by Cooks and co-workers[17] for collisions of the pyrazine molecular ion with a fluorinated surface. This suggested that the ion-surface reaction chemistry of benzene could also be different at fluorinated and alkanethiolate films and prompted our investigation of reactions at the fluorinated surface. In a recent survey of the reactivity of a large number of chemically modified self-assembled monolayer surfaces, Cooks and co-workers detected F addition to benzene and several other related molecular ions;[19] this shows that the reactivity of the fluorinated surface depends on the nature of the projectile ion. For comparison with our experimental results, experimental heats of formation and the results of *ab initio* quantum mechanical calculations are used to predict the energetics of loss of H and H_2 from selected ion-surface reaction adducts.

It has been noted that energy deposition and total scattered ion abundance are higher for a fluorinated surface than for a nonfluorinated surface.[17,19] To provide further insight into ion loss by neutralization at the surface, the results of total ion abundance and surface current measurements are also presented and discussed for the different surface compositions and for different chain lengths of the alkanethiolates.

Results and Discussion

Spectra of Benzene and Benzene-d_6 on *n*-Alkanethiolate Surfaces. Figure 1 shows the spectra obtained for 30- and 70-eV collisions of the benzene molecular ion (m/z 78) with a surface prepared from octadecanethiol. The spectra show the expected[39] dissociation products of benzene (e.g., m/z 27, 39, 50–53, 63, 77), with more extensive fragmentation detected at the higher collision energy. Ions that are not expected dissociation products of $C_6H_6^{•+}$ are also evident from Figure 1 (e.g., m/z 91, m/z 65, and m/z 79 ($C_6H_7^+$)). Although these ions are of low intensity (less than 10% of the total ion abundance), their appearance gives important information on ion-surface reactions and chemical sputtering. Ions at m/z 91 and 65 were detected by Cooks and co-workers in experiments performed on stainless steel and other surfaces and were suggested to correspond to the addition of a methyl group followed by loss of H_2 and then loss of C_2H_2 (Scheme I).[1,4,5] To further explore the reaction in Scheme I, and to determine whether the source of the added CH is adventitious hydrocarbon or the self-assembled monolayer film, we performed deuterium labeling studies.

Scheme I

$$C_6H_6 \xrightarrow{+CH_3} C_7H_9(93) \xrightarrow{-H_2} C_7H_7(91) \xrightarrow{-C_2H_2} C_5H_5(65)$$
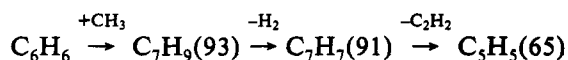
Labeling Studies of Reactions with the Self-Assembled Monolayer Films. Spectra were obtained for the reactions of ionized benzene and benzene-d_6 with self-assembled monolayer films prepared from octadecanethiol and perdeuterioeicosanethiol; the appropriate reaction regions for a collision energy of 30 eV are

(23) Nuzzo, R. G.; Dubois, L. H.; Allara, D. L. *J. Am. Chem. Soc.* **1990**, *112*, 558.

(24) Whitesides, G. M.; Laibinis, P. E. *Langmuir* **1990**, *6*, 87.

(25) Alves, C. A.; Smith, E. L.; Porter, M. D. *J. Am. Chem. Soc.* **1992**, *114*, 1222.

(26) (a) Chidsey, C. E. D.; Loiacono, D. N. *Langmuir* **1990**, *6*, 682. (b) Chidsey, C. E. D.; Bertozzi, C. R.; Putvinski, T. M.; Mujsce, A. M. *J. Am. Chem. Soc.* **1990**, *112*, 4301.

(27) (a) Frisbie, C. D.; Martin, J. R.; Duff, R. R.; Wrighton, M. S. *J. Am. Chem. Soc.* **1992**, *114*, 7142. (b) Li, Y.; Huang, J.; McIver, R. T.; Hemminger, J. C. *J. Am. Chem. Soc.* **1992**, *114*, 2428.

(28) Li, T. T.-T.; Weaver, M. J. *J. Am. Chem. Soc.* **1984**, *106*, 6107.

(29) Rubinstein, I.; Steinberg, S.; Tor, Y.; Shanzer, A.; Sagiv, J. *Nature* **1988**, *332*, 426.

(30) Finklea, H. O.; Avery, S.; Lynch, M.; Furtsch, T. *Langmuir* **1987**, *3*, 409.

(31) Finklea, H. O.; Snider, D. A.; Fedyk, J. *Langmuir* **1990**, *6*, 371.

(32) Finklea, H. O.; Hanshew, D. D. *J. Am. Chem. Soc.* **1992**, *114*, 3173.

(33) Bryant, M. A.; Pemberton, J. E. *J. Am. Chem. Soc.* **1991**, *113*, 3629.

(34) Laibinis, P. E.; Whitesides, G. M.; Allara, D. L.; Tag, Y.-T.; Parikh, A. N.; Nuzzo, R. G. *J. Am. Chem. Soc.* **1991**, *113*, 7152.

(35) Swalen, J. D.; Allara, D. L.; Andrade, J. D.; Chandross, E. A.; Garoff, S.; Israelachvili, J.; McCarthy, T. J.; Murray, R.; Pease, R. F.; Rabolt, J. F.; Wynne, K. J.; Yu, H. *Langmuir* **1987**, *3*, 932.

(36) (a) Nuzzo, R. G.; Allara, D. L. *J. Am. Chem. Soc.* **1983**, *105*, 4481. (b) Allara, D. L.; Nuzzo, R. G. *Langmuir* **1985**, *1*, 45.

(37) Tillman, N.; Ulman, A.; Penner, T. L. *Langmuir* **1989**, *5*, 101.

(38) Cohen, S. R.; Naaman, R.; Sagiv, J. *Phys. Rev. Lett.* **1987**, *58*, 1208.

(39) Rosenstock, H. M.; Dannacher, J.; Liebman, J. F. *Radiat. Phys. Chem.* **1982**, *20*, 7.

(40) March, J. *Advanced Organic Chemistry*, 2nd ed.; McGraw-Hill: New York, 1977.

(41) Carey, F. A.; Sundberg, R. J. *Advanced Organic Chemistry*; Plenum Press: New York, 1977; Parts A and B.

Reactive Collisions of $C_6H_6^{•+}$ and $C_6D_6^{•+}$
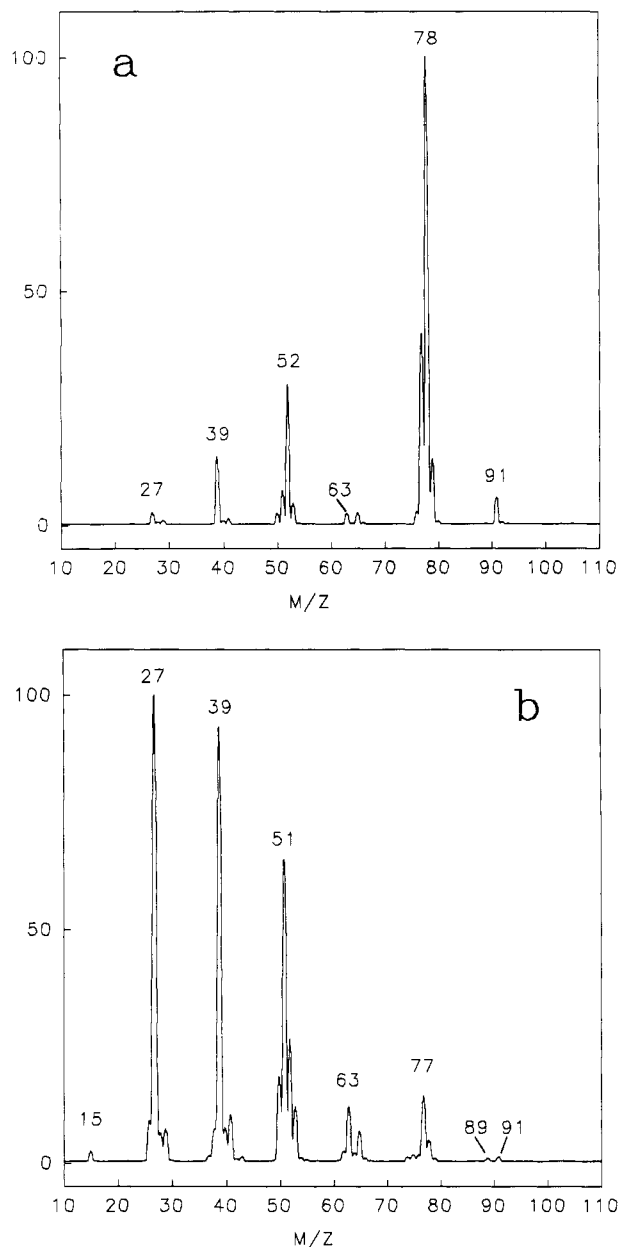
J. Am. Chem. Soc., Vol. 115, No. 12, 1993 5277

Figure 1. Ion-surface collision spectra obtained by colliding benzene molecular ion at (a) 30-eV and (b) 70-eV collision energies with a surface prepared from n-octadecanethiol on vapor-deposited gold.
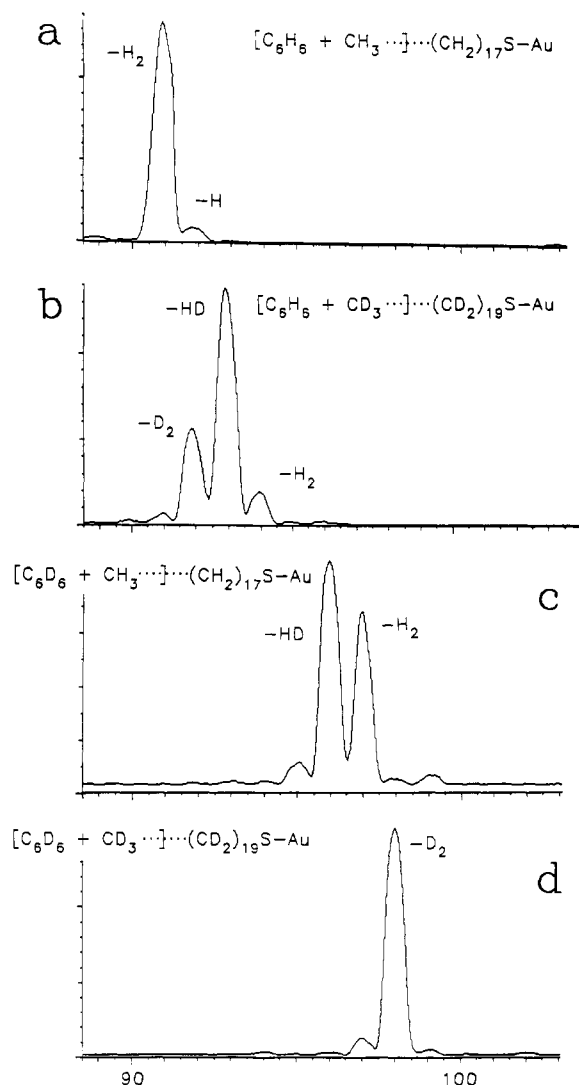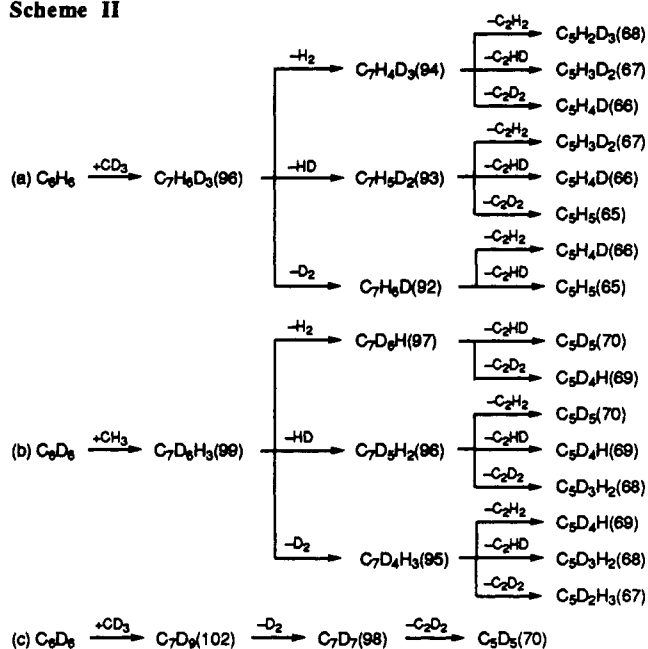

Figure 2. Ion-surface collision spectra in the methyl reaction region obtained by 30-eV collisions of (a) benzene molecular ion with a surface prepared from n-$C_{18}H_{37}SH$, (b) benzene molecular ion with a surface prepared from n-$C_{20}D_{41}SH$, (c) benzene-d_6 molecular ion with a surface prepared from n-$C_{18}H_{37}SH$, and (d) benzene-d_6 molecular ion with a surface prepared from n-$C_{20}D_{41}SH$ (all on vapor-deposited gold).

illustrated in Figure 2. (Complete spectra are available in Figure 1a and as supplementary material.) The peaks of interest shift by an appropriate number of mass units to confirm reactions with the self-assembled monolayer films and not with adventitious hydrocarbons that serve as reaction partners when untreated metals are used. In each case, a minor peak is detected that directly corresponds to methyl addition. However, the major reaction products are consistent with addition of methyl followed by loss of either H_2, HD, and/or D_2, depending on the projectile ion and the surface involved (Scheme II). In each case, further fragmentation by loss of acetylene is also evident from the spectra (e.g., m/z 91 $\rightarrow$ m/z 65; Schemes I and II).

For ionized benzene reacting with the perdeuterio surface (Scheme IIa, Figure 2b), ion-surface reaction products correspond to the addition of CD_3 (m/z 96) followed by loss of H_2 (m/z 94), HD (m/z 93), and D_2 (m/z 92). For benzene-d_6 reacting with the octadecanethiolate surface (Scheme IIb, Figure 2c), three ions are present that formally correspond to a C_1 addition. These ions are m/z 97, 96, and 95, which are consistent with addition of CH_3 followed by loss of H_2, HD, and D_2 (Figure 2c). The

peak corresponding to mixed H_2 loss, i.e., one H (D) atom from the phenyl ring and one H (D) atom from the methyl group (HD, Figure 2b,c), is more intense than those corresponding to H_2 (D_2) loss from the methyl group or H_2 (D_2) loss from the ring. For reaction between $C_6D_6^{•+}$ and the perdeuterio surface, the dominant reaction product (m/z 98) corresponds to addition of CD_3 followed by loss of D_2 (Scheme IIc, Figure 2d). At higher collision energies (>50 eV), subsequent and enhanced losses of H, D, H_2, HD, and D_2 can be observed from the initial CH_3 (CD_3) addition products. Fragmentation of m/z 91 and fragmentation of adducts of higher masses (see below) also contribute to the ion abundances in the low mass portion of the higher energy spectra. For example, the ion of m/z 27 that is detected in the 70-eV dissociation spectrum of ionized benzene-d_6 with the octadecanethiolate surface contains three hydrogens[42] and cannot result simply from the fragmentation of $C_6D_6^{•+}$. Reaction pathways analogous to those in Schemes I and II, but initiated by H addition or addition of alkyl groups larger than methyl, also occur and are sensitive to the chain length of the alkanethiolate (see below).

---

(42) An ion of m/z 27 could also consist of C_2DH, but the analogous product, C_2H_2, is of low relative abundance in the surface collision spectrum of $C_6H_6^{•+}$ with the unlabeled octadecanethiolate surface.

Scheme II

(a) C_6H_6 $\xrightarrow{+CD_3}$ $C_7H_6D_3(96)$
 $\xrightarrow{-H_2}$ $C_7H_4D_3(94)$
  $\xrightarrow{-C_2H_2}$ $C_5H_2D_3(68)$
  $\xrightarrow{-C_2HD}$ $C_5H_3D_2(67)$
  $\xrightarrow{-C_2D_2}$ $C_5H_4D(66)$
 $\xrightarrow{-HD}$ $C_7H_5D_2(93)$
  $\xrightarrow{-C_2H_2}$ $C_5H_3D_2(67)$
  $\xrightarrow{-C_2HD}$ $C_5H_4D(66)$
  $\xrightarrow{-C_2D_2}$ $C_5H_5(65)$
 $\xrightarrow{-D_2}$ $C_7H_6D(92)$
  $\xrightarrow{-C_2H_2}$ $C_5H_4D(66)$
  $\xrightarrow{-C_2HD}$ $C_5H_5(65)$

(b) C_6D_6 $\xrightarrow{+CH_3}$ $C_7D_6H_3(99)$
 $\xrightarrow{-H_2}$ $C_7D_6H(97)$
  $\xrightarrow{-C_2HD}$ $C_5D_5(70)$
  $\xrightarrow{-C_2D_2}$ $C_5D_4H(69)$
 $\xrightarrow{-HD}$ $C_7D_5H_2(96)$
  $\xrightarrow{-C_2H_2}$ $C_5D_5(70)$
  $\xrightarrow{-C_2HD}$ $C_5D_4H(69)$
  $\xrightarrow{-C_2D_2}$ $C_5D_3H_2(68)$
 $\xrightarrow{-D_2}$ $C_7D_4H_3(95)$
  $\xrightarrow{-C_2H_2}$ $C_5D_4H(69)$
  $\xrightarrow{-C_2HD}$ $C_5D_3H_2(68)$
  $\xrightarrow{-C_2D_2}$ $C_5D_2H_3(67)$

(c) C_6D_6 $\xrightarrow{+CD_3}$ $C_7D_9(102)$ $\xrightarrow{-D_2}$ $C_7D_7(98)$ $\xrightarrow{-C_2D_2}$ $C_5D_5(70)$

Reactivity as a Function of Alkanethiolate Chain Length. Long-chain alkanethiols are known to form more highly ordered, crystalline-like surfaces than short-chain alkanethiols.[20,22] A chain length of at least 10 carbons[22] is thought to be required to ensure a highly ordered structure. It is therefore desirable to determine whether ion-surface collision spectra vary with the chain length of the alkanethiol used to prepare the self-assembled monolayer film and, thus, with the crystallinity of the films. Spectra were obtained on four different hydrocarbon surfaces: untreated stainless steel and self-assembled monolayers prepared from

Table I. Relative Intensities of the Most Informative Peaks in the 30-eV Ion-Surface Collision Spectra of Benzene Molecular Ion

m/z	SS	C4 30 h	C4 100 h	C12 30 h	C12 100 h	C18 30 h	C18 100 h
Normalization to Total Ion Abundance[a]							
91	1	1	1	3	3	3	3
79	5	8	10	6	7	6	7
78	17	23	30	43	48	44	48
77	28	31	25	20	21	18	19
(79:78)[b]	(0.29)	(0.35)	(0.33)	(0.14)	(0.15)	(0.14)	(0.15)
(77:78)[b]	(1.7)	(1.3)	(0.83)	(0.47)	(0.44)	(0.41)	(0.40)
65	1	0.6	0.4	1	0.6	1	1
63	2	2	2	1	1	1	1
53	5	3	2	2	2	2	2
52	14	13	15	13	11	13	11
51	10	8	6	3	2	3	2
50	2	2	2	1	1	1	1
43	0.6	0.2	0.1	0.0	0.0	0.0	0.0
39	9	6	6	5	4	6	4
27	5	2	1	1	0.4	1	1
Normalization to Most Intense Peak[c]							
105	5	5	3	1	1	2	1
104	3	2	1	0.4	0.2	0.4	0.3
103	7	6	3	1	1	2	1
93	3	2	5	2	2	2	3
92	10	9	10	8	10	8	11
91	100	100	100	100	100	100	100
90	4	2	2	1	2	1	4
89	4	3	2	2	2	2	2

[a] Relative intensities are normalized to the total ion abundance. Values less than 0.05% are regarded as 0.0. Values 30 and 100 h refer to the time of exposure of the solid electrode to alkanethiol solution. [b] The [m/z 77]/[m/z 78] and [m/z 79]/[m/z 78] intensity ratios are given in parentheses. [c] Relative intensities normalized to the most intense peak (m/z 91) of the reaction region. In this case, spectra were recorded by scanning the second quadrupole in the range m/z 85–150 and using a higher multiplier voltage than for recording full-range (m/z 10–150) spectra.
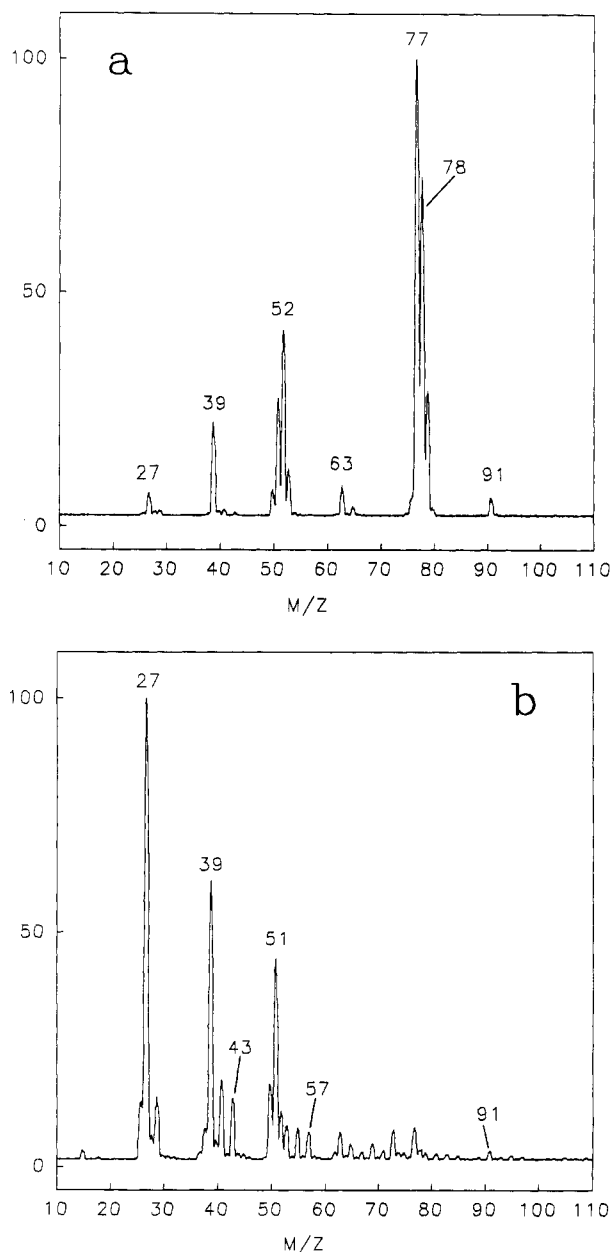
Figure 3. Ion-surface collision spectra obtained by colliding benzene molecular ion at (a) 30-eV and (b) 70-eV collision energies with a surface prepared from n-butanethiol on vapor-deposited gold.

n-butanethiol, n-dodecanethiol, and n-octadecanethiol (hereafter denoted by SS, C_4, C_{12}, and C_{18}, respectively). Relative intensities obtained with the different surfaces are summarized in Table I, and spectra obtained for 30- and 70-eV collisions of ionized benzene with a C_4 surface are illustrated in Figure 3. It is clear from the data in Table I, and from a comparison of Figures 1 and 3, that the spectra change in a manner that is dependent on chain length. The time of exposure of the gold electrode to the alkanethiol solution also affects the spectra obtained with the short-chain alkanethiolate, although it has less influence on the spectra obtained with the longer chain alkanethiolates. Three characteristic differences between the spectra obtained on long- and short-chain alkanethiolate surfaces will be discussed here: (i) the variation in the intensity ratios of [m/z 77]/[m/z 78] and [m/z 79]/[m/z 78], (ii) the percent relative abundance of the ions at m/z 43 and 57, and (iii) the intensity ratio of ions that correspond to addition of methyl and addition of ethyl (see Table I).

The intensity ratio of [m/z 77]/[m/z 78] (see Table I) is greater than unity for stainless steel and for the C_4 surface prepared

Reactive Collisions of $C_6H_6^{\bullet+}$ and $C_6D_6^{\bullet+}$

J. Am. Chem. Soc., Vol. 115, No. 12, 1993 5279

with the short solution exposure time ($[m/z\ 77]/[m/z\ 78] = 1.7$ and 1.3, respectively), close to unity (0.80) for the C_4 alkanethiolate surface prepared with the long exposure time, but significantly less than unity for the C_{12} and C_{18} alkanethiolate surfaces (about 0.4 for both surfaces). Labeling data provide insight into the origin(s) of the ion at $m/z\ 77$ (for spectra, see the supplementary material). In the 30-eV spectrum of $C_6D_6^{\bullet+}$ ($m/z\ 84$) with the *n*-octadecanethiolate surface, the appearance of an ion at $m/z\ 81$ cannot be explained by direct loss of D or D_2 from $C_6D_6^{\bullet+}$ and must involve an initial H addition to C_6D_6, as suggested in Scheme III. The origins of $m/z\ 77$ indicated by the labeling results are $[C_6H_6-H]$ and $[C_6H_7-H_2]$.

Experimental heats of formation[43] can be used to calculate the heats of reaction for H loss from the benzene molecular ion ($C_6H_6^{\bullet+} - H \rightarrow C_6H_5^+$, 91.6 kcal/mol) and for formation of [M + H]$^+$ with subsequent H_2 loss ($C_6H_6^{\bullet+} + RH \rightarrow R^{\bullet} + C_6H_7^+$, $C_6H_7^+ - H_2 \rightarrow C_6H_5^+$, 87.8 kcal/mol; for a C_4 model system R = C_4H_9). The comparable values for these two processes suggest that both reactions can take place, assuming that there are no large barriers to the reactions. The experimental data support this assumption. Because a percentage of the intensity of the ion at $m/z\ 77$ is the result of H addition to benzene with subsequent H_2 loss, the ratio of $[m/z\ 77]/[m/z\ 78]$ can serve as an indicator of the H-donating ability or H-reactivity of the surface. The ion at $m/z\ 77$ increases in relative abundance as the chain length of the alkanethiolate decreases. Another measure of the H-donating ability of the surface is the ratio of $[m/z\ 79]/[m/z\ 78]$. This ratio is 0.29 for stainless steel, 0.35 for C_4, 0.14 for C_{12}, and 0.14 for C_{18} surfaces.

The ratios $[m/z\ 77]/[m/z\ 78]$ and $[m/z\ 79]/[m/z\ 78]$ suggest that the amount of H addition that is detected when benzene collides with the self-assembled monolayer films may be sensitive to the degree of surface disorder; i.e., the more disordered short-chain alkanethiolate surfaces may expose more H in orientations appropriate for H addition than would the crystalline-like surfaces of the long-chain alkanethiolates. The more disordered surfaces might also lead to an increase in the adsorption or insertion of adventitious hydrocarbons at the surface in a manner dependent on the chain length; this could provide a source of reactive hydrogen that would still yield results that are sensitive to chain length. The presence of trace adventitious hydrocarbon is indicated by the appearance of a minor peak at $m/z\ 85$ in the spectrum that results from collisions of $C_6D_6^{\bullet+}$ with the perdeuterated alkanethiolate surface. Reaction at short-chain perdeuterated alkanethiolate films is required to distinguish between these possibilities; these experiments will be performed in subsequent investigations after synthesis of the appropriate perdeuterated thiols.

Scheme III
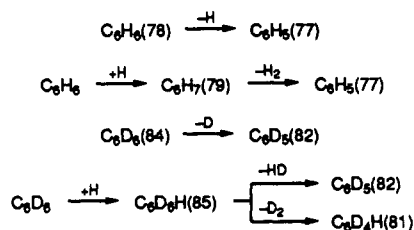
The relative abundances of the ions at $m/z\ 43$ and 57 are of interest because they vary with the chain lengths of the alkanethiols used to prepare the films (compare Figures 1b and 3b). These ions cannot be direct dissociation products of $C_6H_6^{\bullet+}$ because they contain seven hydrogens ($C_3H_7^+$) and nine hydrogens

($C_4H_9^+$), respectively.[45] The ions of $m/z\ 43$ are either dissociation products of $m/z\ 79$ (the H addition product of benzene) or alkyl ions that are sputtered from the surface; chemical sputtering involves electron transfer from the surface to the projectile with the release of ionized surface species. At 30-eV collision energy, the abundance of $m/z\ 43$ (or $m/z\ 50$) relative to the total abundance of all ions is <0.05% when the C_{18} (or perdeuterio C_{20}) thiol surfaces are used, but approximately 0.2% when the shorter chain surfaces are utilized (Table I). The ion of $m/z\ 57$ is either a dissociation product of a higher order adduct (e.g., $[C_6H_6 + CH_3]^+ \rightarrow [C_4H_9^+]$) or an alkyl ion that is sputtered directly from the surface. The formation of $C_3H_7^+$ ($m/z\ 43$) from $C_6H_7^+$ or formation of $C_4H_9^+$ ($m/z\ 57$) from $C_7H_9^+$ would require extensive skeletal reorganization, suggesting that these pathways are unlikely. It seems more reasonable that these ions, and several other ions apparent from Figure 3b but not Figure 1b, are the result of chemical sputtering of either the hydrocarbon chain of the alkanethiolate or adventitious hydrocarbons adsorbed onto, or inserted into, the chemisorbed alkanethiolate film. The possibility that adventitious hydrocarbons are adsorbed onto, or inserted into, the films prepared from the shorter chain alkanethiol is supported by the detection of $m/z\ 57$ ($C_4H_9^+$) when benzene collides with a C_2 alkanethiolate surface.[46] $C_2H_5^+$ would be the largest alkyl ion that can be directly sputtered from a single ethanethiolate chain. Sputtering involving more than one alkanethiolate chain from ethanethiolate, e.g., $C_2H_5 + C_2H_5$, is intuitively less probable, but cannot be ruled out.

The 30-eV spectra for benzene molecular ion colliding with alkanethiolate surfaces show peaks corresponding to CH_3 addition, e.g., $m/z\ 93, 91, 89$, as well as peaks at higher masses, e.g., $m/z\ 105, 103$ (Table I). Ions of these m/z values are consistent with the following processes: $C_6H_6 + CH_3 \rightarrow C_7H_9$ ($m/z\ 93$), $93 - H_2 \rightarrow 91$, $91 - H_2 \rightarrow 89$; $C_6H_6 + C_2H_5 \rightarrow C_8H_{11}$ ($m/z\ 107$), $107 - H_2 \rightarrow 105$, $105 - H_2 \rightarrow 103$. Although some amount of the ion at $m/z\ 91$ could correspond to the fragmentation of higher alkyl adducts (e.g., ethyl addition–CH_4), the intensity ratio $[89 + 91 + 93]/[103 + 105 + 107]$ varies with chain length and is used as a measure of the relative amount of methyl/ethyl addition.[47] A value for this ratio of greater than 25:1 was obtained for C_{12} and C_{18} surfaces regardless of solution exposure time. In contrast, a value of less than 10:1 was obtained for the C_4 surface exposed for 30 h and for the stainless steel surface. A possible explanation for this is that the more ordered C_{12} and C_{18} surfaces mainly expose methyl groups for reaction with the incoming projectiles. The shorter chain, more disordered alkanethiolate surfaces have more gauche interactions and thus also allow the addition of an ethyl group. Another possibility is that, as mentioned above, more adventitious hydrocarbon is accessible on the less ordered C_4 surface, which could also lead to an increase in ethyl addition relative to that detected for the ordered, low free energy surfaces composed of long-chain alkanethiolates.

(45) An ion of $m/z\ 43$ could also have the molecular formula C_2H_3O. In our data, $C_3H_7^+$ seems more likely because larger alkyl ions, C_nH_{2n+1}, and their dissociation products, C_nH_{2n-1} and C_nH_{2n-3} are often detected.

(46) Callahan, J. H.; Ding, J.-M.; Wysocki, V. H. Unpublished results.

(47) We suggest that fragmentation of the higher mass adducts (e.g., the ion corresponding to ethyl addition) can contribute to the ion abundance at $m/z\ 91$ (formal methyne addition, $[+CH_3 - H_2] = [+CH]$). Gas-phase experiments support the view that the formal CH addition can arise from addition of larger alkyl groups. Although ionized benzene is known to be unreactive with alkanes,[48] benzene added to a chemical ionization plasma of isobutane (neutral benzene reacting with ionized hydrocarbon) forms adducts that correspond to alkyl ion addition to benzene.[46] If one of these adducts, such as $[C_6H_6 + C_3H_7]^+$, is then mass-selected and allowed to collide with a target gas (Ar) or a surface, a fragment ion of $m/z\ 91$ is detected. The contribution of higher mass adducts to the abundance at $m/z\ 91$ should not preclude the use of the ratio [methyl addition]/[ethyl addition] as an indicator of surface order. The variation of this ratio with chain length is experimentally observable, and labeling data acquired at higher collision energies show that an increase in the percentage of $m/z\ 91$ that results from addition of alkyl groups larger than methyl is accompanied by an increase in the amount of detectable higher mass addition products.

(48) Gross, M. L.; Russell, D. H.; Aerni, R. J.; Bronczyk, S. A. *J. Am. Chem. Soc.* 1977, 99, 3603.

(43) ΔH_f (experimental, from ref 44): C_6H_6, 19.8; $C_6H_6^{\bullet+}$, 233.2; $C_6H_7^+$ 204.1 (PA benzene 181.3); $C_6H_5^+$, 272.8; C_4H_{10}, −30.2; C_4H_9,18; H, 52.0; H_2, 0 kcal/mol.

(44) Lias, S. G.; Bartmess, J. E.; Liebman, J. F.; Holmes, J. L.; Levin, R. D.; Mallard, W. G. *J. Phys. Chem. Ref. Data* 1988, *17*, Suppl. 1.
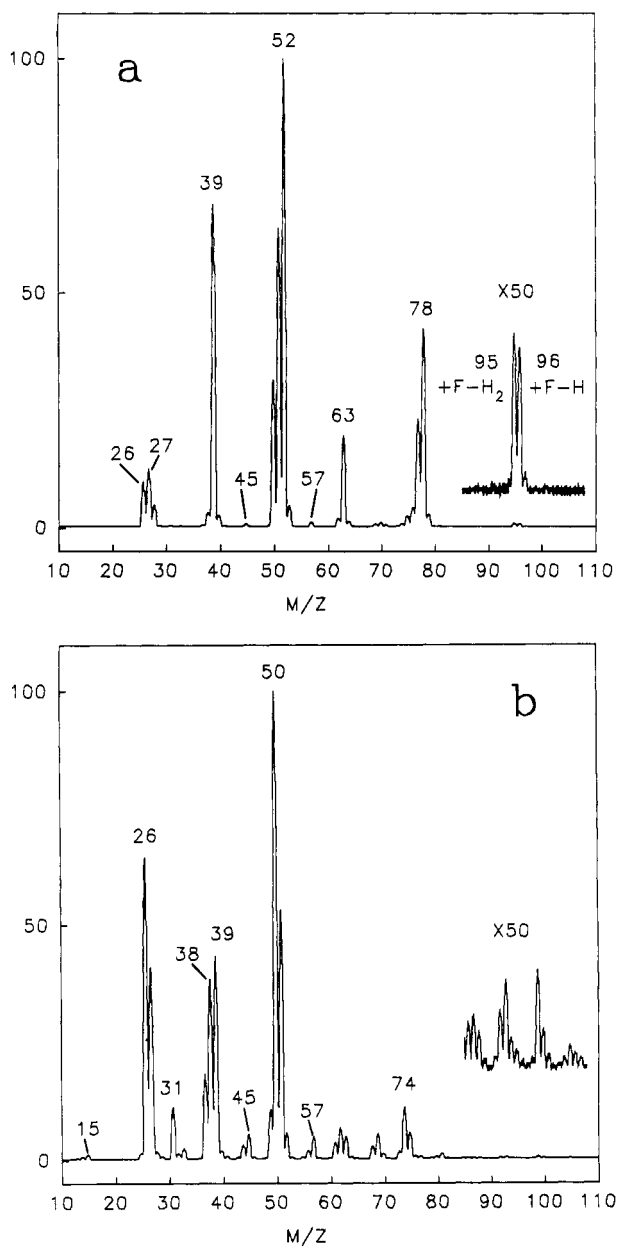
Figure 4. Ion-surface collision spectra obtained by colliding benzene molecular ion at (a) 30-eV and (b) 70-eV collision energies with a surface prepared from 2-(perfluorooctyl)ethanethiol on vapor-deposited gold.

Spectra of Benzene, Benzene-d_6 and Fluorobenzene on $CF_3(CF_2)_7CH_2CH_2SAu$. The spectra of the benzene molecular ion (m/z 78) colliding with the fluorinated surface ($CF_3(CF_2)_7$-CH_2CH_2SAu) at collision energies of 30 and 70 eV are given in Figure 4. At a given collision energy, the relative abundance of low mass fragments is greater than is detected for ions colliding with the alkanethiolate surfaces (see, for example, Figure 1). This suggests that greater energy is deposited upon collision with the fluorinated surface. These results are in agreement with those reported for pyrazine,[17,19] as well as our recent results for doubly charged buckminsterfullerene, C_{60}^{2+}. Dramatically enhanced fragmentation is observed for C_{60}^{2+} upon collision with the fluorinated surface but not with the octadecanethiolate surface.[49] The intensities of the benzene fragments of lower m/z ratios, i.e., with higher energy requirements for dissociation, increase with increasing collision energy (see, for example, the intensity ratios of peaks at m/z 50/51, 38/39, 26/27), and the molecular ion is almost negligible at higher collision energies (greater than 50

eV). Note that the abundant fragment ion at m/z 26 in Figure 4 is not observed in the spectra obtained by collision of ionized benzene with hydrocarbon surfaces (compare Figure 4 with Figures 1 and 3).

The appearance of the peaks at m/z 96 and 95 in Figure 4a is also important. The origin of these peaks is most readily explained by assuming reaction between the benzene molecular ion and the fluorinated chain of the surface; the formation of ions of m/z 96 and 95 can be initiated by fluorine addition followed by loss of H and H_2, respectively. The appearance of these peaks has also been noted in a parallel and independent investigation.[19] Peaks at higher masses, m/z 127 and 145, are also observed in the 30-eV spectrum of benzene molecular ion with the fluorinated surface. The origin of these ions is presumably an initial CF_3 addition followed by the loss of HF or H_2. These assumptions are supported by measurements made with benzene-d_6; the peaks at m/z 95 (C_6H_4F), 96 (C_6H_5F), 127 ($C_7H_5F_2$), and 145 ($C_7H_4F_3$) are shifted to m/z 99 (C_6D_4F), 101 (C_6D_5F), 132 ($C_7D_5F_2$), and 149 ($C_7D_4F_3$), respectively.

Many of the same peaks, e.g., m/z 50, 39, 38, 27, 26, are present in both the benzene (Figure 4) and fluorobenzene (supplementary material) ion-surface collision spectra. For benzene, it cannot be excluded that some percentage of these fragments originates from the fragmentation of the ion-surface reaction products, e.g., m/z 97, 96, and 95, and not from the benzene molecular ion. The ions at m/z 70, 57, and 45 can be interpreted as fluorinated analogues of the fragments $C_4H_4^{\cdot+}$, $C_3H_3^+$, and $C_2H_3^+$, i.e., $C_4H_3F^{\cdot+}$, $C_3H_2F^+$, and $C_2H_2F^+$, respectively, as supported by their shifts to m/z 73, 59, and 47, respectively, for benzene-d_6. The peaks at m/z 31 and 69 in the benzene spectra presumably correspond to the ions CF^+ and CF_3^+, respectively. The relative abundances of the fluorine-containing ions increase in intensity with increasing collision energy (compare Figure 4a with 4b). It is also of interest that the fluorobenzene molecular ion adds fluorine and CF_3 as well, although the intensity ratio of the $[M + F - H]^{\cdot+}$ and $[M + F - H_2]^+$ ions ($[m/z$ 114]/$[m/z$ 113]) is significantly greater than unity, in contrast to the $[m/z\,96]/[m/z\,95]$ ratio detected for the reaction of benzene molecular ion with the fluorinated surface.

Finally, we note that a peak at m/z 91 is sometimes present in the spectra obtained by using a fluorocarbon surface. As discussed above, an ion of this m/z always appears in the benzene spectra obtained with alkanethiolate surfaces, and it results from the formal addition of CH to the benzene molecular ion. Its appearance indicates the presence of hydrocarbons on the fluorocarbon surface and has been found to depend on the surface preparation. The lowest abundance (0%) of m/z 91 is detected when the fluorocarbon surface is prepared on plasma-cleaned, vapor-deposited gold. A greater abundance of m/z 91 is observed when vapor-deposited gold is used with no plasma cleaning; a still greater abundance is observed when mechanically polished gold foil is used. The ratio of the peaks $[m/z\,91]/[m/z\,95 + m/z\,96]$ also increases slowly with time, suggesting that as the surface is damaged by F removal hydrocarbon is adsorbed. When the ion of m/z 91 becomes more abundant than m/z 95 or 96, the extent of fragmentation is still greater than that detected on an alkanethiolate surface; i.e., the surface still behaves as a predominantly fluorocarbon surface in terms of the amount of kinetic energy converted to internal energy of the projectile upon collision.

Notes on H, F, and CH_3 Adduct Ions and Their Subsequent Fragments. For comparison with our experimental results, *ab initio* quantum chemical calculations have been carried out on several structures that correspond to the proposed products of ion-surface reactions between benzene molecular ion and hydrocarbon or fluorocarbon surfaces. These ions include addition products, e.g., ipso-$C_6H_7^+$ (m/z 79), ipso-$C_6H_6F^+$ (m/z 97), and ipso-$C_6H_6(CH_3)^+$ (m/z 93), and some of their fragments, such

(49) Callahan, J. H.; Somogyi, Á.; Wysocki, V. H. Manuscript in preparation.

Reactive Collisions of $C_6H_6{}^{\bullet+}$ and $C_6D_6{}^{\bullet+}$

J. Am. Chem. Soc., Vol. 115, No. 12, 1993 5281

Table II. Relative Energies of the H and H_2 Losses from H, F, and CH_3 Addition Products of Benzene[a]

reaction	relative energies[b]
H addition	
ipso-$C_6H_7{}^+ \rightarrow C_6H_6{}^{\bullet+} + H$	65.5 [81.1][c]
ipso-$C_6H_7{}^+ \rightarrow C_6H_5{}^+ + H_2$	52.0 [68.7][c]
$C_6H_6{}^{\bullet+} \rightarrow C_6H_5{}^+ + H$	95.8 [91.6][c]
F addition	
ipso-$C_6H_5F^+ \rightarrow C_6H_5F^{\bullet+} + H$	48.1
ipso-$C_6H_5F^+ \rightarrow p\text{-}C_6H_4F^+ + H_2$	43.5 [45.1]
$C_6H_5F^{\bullet+} \rightarrow p\text{-}C_6H_4F^+ + H$	104.6
CH_3 Addition	
ipso-$C_6H_6(CH_3)^+ \rightarrow C_6H_5CH_2{}^+ + H_2$	5.8[d]
ipso-$C_6H_6(CH_3)^+ \rightarrow$ ipso-$C_6H_6CH^+ + H_2$	94.0

[a] Total energies calculated at the 6-31G//6-31G SCF, 6-31G*//6-31G SCF, and MP2 6-31G//6-31G SCF levels, 3-21G zero-point vibrational energies, and experimental heats of formation are given in Table S1 of the supplementary material. [b] Relative energy calculations are based on total energies calculated at the 6-31G*//6-31G SCF level, on the Hartree–Fock limit for H (−0.5 hartree), and on the experimental total energy for H_2,[56] unless otherwise noted. [c] Values calculated from experimental heats of formation. [d] The formation of the cyclo-$C_7H_7{}^+$ (tropylium) cation can be predicted to be slightly exothermic; the corresponding value is −6.3 kcal/mol.

as $C_6H_6{}^{\bullet+}$ (m/z 78), $C_6H_5{}^+$ (m/z 77), $C_6H_5F^{\bullet+}$ (m/z 96), $C_6H_4F^+$ (m/z 95), $C_6H_5CH_2{}^+$ (m/z 91), and ipso-$C_6H_6CH^+$ (m/z 91). Relative energy levels calculated for the losses of H and H_2 from the H, F, and CH_3 adduct ions are given in Table II. Total energies obtained by 6-31G//6-31G, 6-31G*//6-31G SCF, and MP2 6-31G//6-31G SCF calculations, 3-21G zero-point vibrational energies, and the available experimental heats of formation of the investigated species are collected in Table S1 of the supplementary material. A more detailed treatment of the various ion-surface interactions will be presented elsewhere.

(i) H or F Addition with Subsequent Fragmentation. Hydrogen addition to the benzene molecular ion presumably leads to a σ-complex $C_6H_7{}^+$ cation, which is well-known and has been studied.[50] Unfortunately, the structure and the experimental heat of formation of the analogous F adduct is not known. By analogy with the reaction of neutral benzene with F_2, which leads to ipso-fluorocyclohexadienyl radical (i-$C_6H_6F^{\bullet}$),[51] is is reasonable to assume the formation of an ion having a structure similar to that of the radical. A structure with C_s symmetry was calculated to be a *minimum* on the potential energy surface.[52] Additionally, MNDO bond orders, which have been proved recently to be useful for the description of ion structures and primary fragmentation processes,[18c,53] support that this i-$C_6H_6F^+$ cation has a σ-complex structure. In this structure, both the fluorine and hydrogen atoms are bonded to the C_1 carbon atom, with bond orders of 0.982 for C_1–F and 0.916 for C_1–H.

The losses of the H radical and the H_2 molecule from this i-$C_6H_6F^+$ cation are quite endothermic, by 48.1 and 43.5 kcal/

mol, respectively (Table II).[54] The corresponding values for the analogous $C_6H_7{}^+$ ion are larger, 52.0 and 65.3 kcal/mol, respectively (Table II). As was mentioned above, the peak corrsponding to the intact adduct cation, i-$C_6H_6F^+$ (m/z 97), is of lower intensity than those corresponding to subsequent H (m/z 96) or H_2 (m/z 95) losses (Figure 4a). This suggests that the i-$C_6H_6F^+$ cation (and, presumably, also the $C_6H_7{}^+$ (m/z 79) ion) contains a significant amount of internal energy for subsequent fragmentation (>2 eV) and that this extra energy is available from the collisions. The appearance of the ion at m/z 95 in the reaction region of the SID spectrum of benzene with the fluorinated alkanethiolate surface (Figure 4a) could also result from the loss of H from the ion at m/z 96, the structure of which may be identical to that of the fluorobenzene molecular ion. This process seems unlikely, however, because the [M − H]$^+$ peak (m/z 95) is of low intensity in the fluorobenzene electron impact (EI) and ion-surface collision spectra (supplementary material), and the H loss from the fluorobenzene molecular ion is predicted to be highly endothermic (by 104.6 kcal/mol, Table II). As was mentioned above, the analogous process, the loss of H from the benzene molecular ion is also highly endothermic (>91.6 kcal/mol).

(ii) CH_3 Addition and Subsequent Loss of H_2. The loss of H_2 from an ipso-$C_6H_6(CH_3)^+$ ion could lead, for example, to the benzyl cation ($C_6H_5CH_2{}^+$) or a rearranged tropylium cation, cyclo-$C_7H_7{}^+$, in a process in which one H of the H_2 originates from the CH_3 group, while the other originates from the benzene ring. Another reasonable mechanism is the loss of H_2 from the CH_3 group, which leads to the formation of an ipso-$C_6H_6CH^+$ ion (Table II). The former process, one H from the methyl group and one from the ring, is calculated to be significantly less endothermic, which is in accordance with the experimental observations discussed above (see deuterium labeling results, Figure 2).

Total Scattered Ion Abundance and Surface Current vs Surface Composition. To this point, surface-induced dissociation, ion-surface reactions, and chemical sputtering have been discussed. Another process, neutralization of the projectile ion without the release of detectable charged adsorbates, competes with the above processes and results in the loss of a portion of the incoming ion beam. We describe here attempts to monitor neutralization losses as a function of the surface type. The neutralization is examined in two ways: (i) by measuring the total ion signal at the detector and (ii) by using a picoammeter to continuously monitor the current at the surface.

A typical plot of the total ion signal collected at the detector following 30-eV collisions of $C_6H_6{}^{\bullet+}$ with each of four surfaces is shown in Figure 5. The total scattered ion abundance is found to vary as a function of the chain length of the alkanethiolate and the chemical composition of the self-assembled monolayer, with the fluorocarbon surface giving the highest total ion signal collected at the detector. (Qualitatively, this effect is noticed as the experiments are performed and manifests itself in easier tune-up of the mass spectrometer and shorter required data collection times for the fluorinated surface.) Our results for the current measured *at the surface* are also shown in Figure 5 and vary from 0.21 nA for the fluorinated surface to 0.37 nA for the C_4 surface. These results qualitatively agree with the results of electrochemical studies. Those monolayers that best block electron transfer in

(50) Bader, R. F. W.; Chang, C. *J. Phys. Chem.* **1989**, *93*, 5095.

(51) Grover, J. R.; Wen, Y.; Lee, Y. T.; Shobatake, K. *J. Chem. Phys.* **1988**, *89*, 938.

(52) A detailed and thorough experimental and *ab initio* study on the HF loss from protonated fluorobenzene appeared in the same journal while our manuscript was in press (Hrušák, J.; Schröder, D.; Weiske, T.; Schwartz, H. *J. Am. Chem. Soc.* **1993**, *115*, 2015). Note that although the isomerization of the ipso-$C_6H_6F^+$ cation to the more stable O-isomer cannot be ruled out in our case, it has no effect on our final conclusions.

(53) (a) Császár, A. G.; Somogyi, Á.; Pócsfalvi, G.; Traldi, P. *Org. Mass Spectrom.* **1992**, *27*, 1349. (b) Vékey, K.; Somogyi, Á.; Tamás, J.; Pócsfalvi, G. *Org. Mass Spectrom.* **1992**, *27*, 869. (c) Somogyi, Á.; Gömöry, Á. *Chem. Phys. Lett.* **1992**, *192*, 221. (d) Curcuruto, O.; Favretto, D.; Traldi, P.; Ajo, D.; Cativiela, C.; Mayoral, J. A.; Lopez, M. P.; Fraile, J. M.; Garcia, J. I. *Org. Mass Spectrom.* **1991**, *26*, 977. (e) Somogyi, Á.; Gömöry, Á.; Vékey, K.; Tamás, J. *Org. Mass Spectrom.* **1991**, *26*, 936. (f) Gömöry, Á.; Somogyi, Á.; Tamás, J.; Stájer, G.; Bernáth, G.; Komáromi, I. *Int. J. Mass Spectrom. Ion Processes* **1991**, *107*, 225. (g) Somogyi, Á.; Tamás, J.; Császár, A. G. *J. Mol. Struct. THEOCHEM* **1991**, *232*, 123.

(54) We used the energetic data for the $p\text{-}C_6H_4F^+$ isomer for the H_2 loss product, because it was found to be the most stable isomer by STO-3G,[55] 6-31G//6-31G, and 6-31G*//6-31G SCF calculations. Our MP2 6-31G//6-31G SCF calculations predict the meta isomer to be slightly more stable than the para isomer; the small energy difference (0.3 kcal/mol) between these isomers shows that the selection of the $p\text{-}C_6H_4F^+$ isomer has no significant effect on our conclusions. The ortho isomer is predicted to be less stable by 2.6 kcal/mol than the meta isomer by MP2 6-31G//6-31G SCF calculations.

(55) Dill, J. D.; Schleyer, P. v. R.; Pople, J. A. *J. Am. Chem. Soc.* **1977**, *99*, 1.

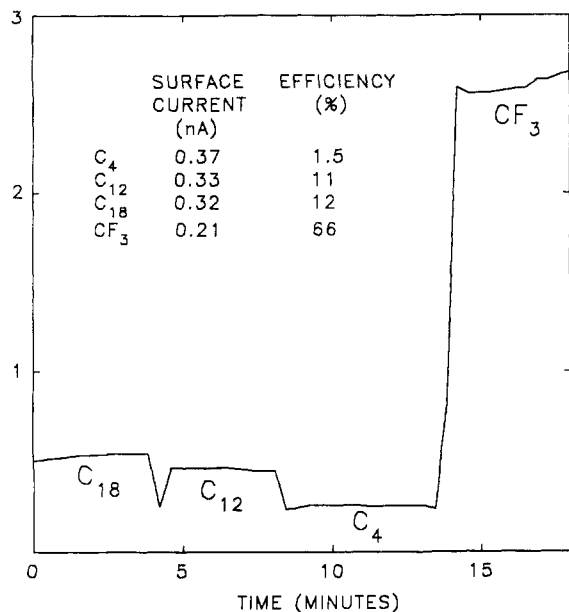(56) Herzberg, G. *J. Mol. Spectrosc.* **1970**, *33*, 147.

Figure 5. Plot showing total ion abundances obtained for 30-eV collisions of benzene molecular ion with four different surfaces. Surface current (nanoamperes) and efficiency (%) values are given in the insert. The surfaces are positioned sequentially into the ion beam path while data are continuously acquired.

solution (fluorinated surface > long-chain alkanethiolate > short-chain alkanethiolate)[20,26a] give the lowest measured current at the surface in our experiments, and those monolayers that are poorer barriers to electron transfer in solution produce higher measured currents at our surface. It is clear from Figure 5 that the total ion signal measured at the detector is low when the current measured at the surface is high, and vice versa. Note here that the trend shown in Figure 5 remained the same at higher (e.g., 70 eV) collision energies, although the absolute values for the total ion abundances increased by about 50% for the alkanethiolate surfaces and by about 100% for the fluorocarbon surface.

The results suggest that the current measured at the surface is a good indicator of the ions lost to neutralization. The lower the current measured at the surface, the better is the surface at yielding a high total scattered ion abundance, i.e., an increased efficiency. The efficiency of the ion-surface collision experiments is defined[1] by $\sum_i I_i / \sum_j I_{trans}$, where $\sum_i I_i$ is the total ion signal detected following collision (i.e., total scattered ion abundance detected) at a given collision energy and $\sum_j I_{trans}$ is the total parent ion signal reflected past the surface without collision. The efficiency is found to improve significantly when the $CF_3(CF_2)_7CH_2CH_2$-SAu surface, rather than the $CH_3(CH_2)_nSAu$ (n = 3, 11, 17) surfaces, is used. Efficiency values measured for 30-eV collisions of benzene molecular ion with C_4, C_{12}, and C_{18} alkanethiolate surfaces and the fluorocarbon surface are 1.5%, 11%, 12%, and 66%, respectively (gold surfaces were exposed to thiol solutions for 100 h). Both total ion current and surface current data show that the monolayers retain the relative electron barrier properties reported for solution,[26a] even after transfer from solution to high vacuum (10^{-7} Torr), i.e., in the absence of solvent.

In principle, there are several sources of the electrons required for the neutralization of the projectile: the gold, the self-assembled monolayer chain(s), and any physisorbed material(s). Relatively large pinholes in the monolayers would be required to allow the benzene molecular ion to penetrate and gain an electron from the gold. In this case, the neutralization can be assumed to be less favorable for highly ordered, thick crystalline surfaces, such as C_{12} and C_{18} alkanethiolates and fluorinated alkanethiolates, than for stainless steel and shorter chain alkanethiolates. The high ionization energies of fluorocarbons lead to the expectation that

neutralization should be decreased at the fluorinated surface, compared with the alkanethiolate surfaces, because charge exchange between the projectile ion and the fluorocarbon is not as energetically favorable as charge exchange between the projectile ion and hydrocarbon (IE benzene = 9.25 eV[44]; IE fluorocarbon, e.g., C_3F_8 = 13.38 eV;[44] IE hydrocarbons, e.g., C_3H_8 = 10.95 eV;[44] $C_{10}H_{22}$ = 9.65[44]). Finally, physisorbed materials (e.g., hydrocarbons from the pump oil) are presumably of higher relative concentration on less ordered, short-chain alkanethiolate films; neutralization by electron transfer to these materials is also in line with the relative order of projectile neutralization described in this section.

The results presented in this section show the importance of the measurements of the total ion signal and surface currents. It is not expected that these experiments will provide a general surface analysis method for a large variety of unknown surfaces. Nevertheless, it is obvious that these experiments provide a means to examine electron-transfer properties between an ion and a modified electrode in the absence of solvent. For the systems investigated here, the gas-phase results are consistent with those obtained in solution.

Conclusions

The results presented in this article clearly show that, upon collision at kinetic energies in the electronvolt range, benzene reacts with alkanethiolate and fluorinated alkanethiolate self-assembled monolayer films. Peaks corresponding to H, CH_3, F, and CF_3 additions, and subsequent H and H_2 losses from the adducts, are observed in the ion-surface collision mass spectra of the benzene molecular ion. The self-assembled monolayer film is the source of the formal CH addition reaction, as illustrated by deuterium labeling results.

6-31G*//6-31G SCF *ab initio* calculations suggest that the F addition product might have an ipso-$C_6H_6F^+$ structure; this is a stable species, i.e., a minimum on the potential energy surface.[52] The H and F adduct ions must have significant internal energy (>2 eV) for subsequent H and H_2 losses, which leads to the peaks observed with higher intensities than those of the intact adduct ions. Both calculations and deuterium labeling results suggest that the loss of H_2 from the CH_3 adduct ion, ipso-$C_6H_6(CH_3)^+$, leads to the stable $C_7H_7^+$ cation.

Ionized benzene serves as a useful probe for the characterization of self-assembled monolayer films inserted into high vacuum (10^{-7} Torr). The data for ionized benzene are sensitive to (i) the chemical composition of the monolayer, (ii) the chain length of the alkanethiol used to prepare the film, (iii) the preparation of the gold surface prior to reaction (mechanically polished gold foil vs vapor-deposited gold vs plasma-cleaned vapor-deposited gold), and (iv) the exposure time between the alkanethiol solution and the gold. For alkanethiolate surfaces (C_nH_mSAu) of varying chain lengths and different surface preparation methods, the data show that the octadecanethiolate surface prepared on plasma-cleaned, vapor-deposited gold produces the lowest [m/z 77]/ [m/z 78] and [m/z 79]/[m/z 78] ratios (i.e., the least H addition), the lowest relative abundance of chemical sputtering products (in comparison with shorter chain alkanethiolates), and the highest ratio of C_1H_x/C_2H_y addition.

The total scattered ion abundance is the greatest from the fluorinated surface, as indicated by measurements of the currents at the surface as well as measurements of the total ion current at the detector (for a given initial ion current of a selected projectile ion). These data provide insight into ion loss by neutralization and suggest that, under vacuum, the relative electron barrier properties of the films are consistent with those reported for electrochemical experiments in solution. Together, the mass spectra and the current measurements show that the relative characteristics of the films as a function of chain length and composition (degree of order, electron barrier properties) are retained upon transfer from solution to vacuum.

As a continuation of the work presented here, we are pursuing several lines of investigation that have been designed to further explore interactions between low-energy ions and self-assembled monolayer films. These experiments involve (i) ion-surface addition reactions with a large variety of even and odd electron projectile ions, (ii) charge exchange between the films and atomic projectile ions of varying ionization energy, and (iii) current measurements at the surface and the detector. These studies may provide further insight into the behavior of self-assembled monolayer surfaces in the gas phase and may allow us to describe those parameters that enhance the desired interaction at a surface.

Experimental Section

The experimental setup has been described.[16] Two Extrel 4000u quadrupoles are positioned at 90° with a surface placed to intersect the ion optical path of the two quadrupoles. For the work presented here, ions were produced by 70-eV electron ionization. The surface can be rotated about the z-axis (Q1 and Q2 in the xy plane). The surface is positioned 45–50° relative to the surface normal. The collision energy is varied by increasing the source potential relative to the surface potential; to transmit ions past the surface without collision, this potential difference is held at approximately 0 eV. The efficiency of the experiments is defined[1] by $\sum_i I_i / \sum_j I_{trans}$, where $\sum_i I_i$ is the total ion current detected following collision (i.e., total scattered ion abundance detected) at a given collision energy and $\sum_j I_{trans}$ is the total parent ion current reflected past the surface without collision.

The alkanethiols were purchased from Aldrich (99%). The perdeuterated thiol was synthesized from the corresponding alkyl bromide ($C_{20}D_{41}Br$, Cambridge Isotope Laboratories; 97% D) and an equimolar amount of thiourea by a standard procedure (refluxing ethanol, hydrolysis with NaOH, acidification with H_2SO_4, extraction with benzene).[57] The fluorinated thiol was prepared by the same procedure from the corresponding iodide ($CF_3(CF_2)_7CH_2CH_2I$, Daikin Chemicals, Japan) and thiourea. Two types of surfaces were used in the experiments, as indicated in the text. Gold foil (0.1 mm thick) was purchased from Aldrich and mechanically polished with alumina (starting with 1.0 μm and working down to 0.05-μm alumina). The vapor-deposited gold surfaces were obtained from Evaporated Metal Films (Ithaca, NY). The surfaces are $^{17}/_{32} \times ^{11}/_{16}$ in. (0.5 mm silica base) and have an underlayer (50 Å) of either titanium or chromium that is covered with 1000-Å vapor-deposited gold. The surfaces were cleaned with an air plasma for 15 min. The surfaces were then immediately immersed into a 20 mM ethanol solution of a given thiol and allowed to react for a minimum of 20 h. In the text, the surfaces prepared from *n*-alkanethiols are referred to as alkanethiolate surfaces or are indicated by the number of carbons in the alkyl chain (e.g., C_{18}). The surface prepared from 2-(perfluorooctyl)ethanethiol is referred to as the fluorocarbon surface.

A novel surface holder has been designed whereby four separate surfaces are aligned vertically at the end of a moveable probe, allowing any of the four surfaces to rest in the path of the ion beam. The holder is a $^{17}/_{32} \times 3 ^1/_4 \times ^1/_{16}$ in. Teflon strip with four shallow grooves to hold the surfaces. Each surface is covered with a stainless steel frame having a 0.5 × 0.5 in. opening (Kimball Physics Inc., Wilton, NH). All four

frames are connected with a single lead to the voltage supply via the back of the holder. For the surface current measurements, each surface is isolated electrically. Surface currents are measured with a Keithley Model 485 picoammeter, connected in series to the power supply/surface circuit. In an attempt to maximize the signal, the number of electrical connections within the circuit was kept at a minimum. Crude Faraday cages, e.g., aluminum foil wrapping, were employed to minimize external noise.

Computational Details. Electronic wave functions were determined by applying the single-configuration, self-consistent-field, restricted Hartree–Fock (SCF) method[58a] and, for closed-shell species, the second-order Møller–Plesset (MP2) perturbation method.[59] (The MP2 method was not available to us for open-shell species.) The following three basis sets were used in our calculations: 3-21G,[60] 6-31G,[61] and 6-31G*.[62] Even-electron ions were assumed to be in their singlet state and odd-electron ions in their doublet states. For open-shell systems the restricted open-shell Hartree–Fock (ROHF) method was applied.[58b] Geometries were fully optimized at the 3-21G SCF and 6-31G SCF levels with the symmetry restrictions given in Table S1 of the supplementary material. Total energies were also determined at the 6-31G SCF optimized geometries by the 6-31G* basis set (referred to as 6-31G*//6-31G SCF) and by the MP2 method (MP2 6-31G//6-31G SCF). To estimate the error on energy calculation caused by the application of 6-31G equilibrium geometries, we carried out 6-31G* SCF geometry optimization on some cations. For example, the 6-31G*//6-31G* SCF energy of the ion i-$C_6H_6F^+$ is calculated to be lower by only 1.3 kcal/mol than that of the 6-31G*//6-31G SCF energy. This energy difference for the ions $C_6H_7^+$ and i-$C_7H_9^+$ is even less, 0.1 kcal/mol for each. Analytical second derivative calculations at the 6-31G SCF level proved to be computationally prohibitive for us; therefore, zero-point vibrational analyses were carried out at the 3-21G SCF level. All *ab initio* calculations were performed using the program package GAMESS.[63]

Supplementary Material Available: Figures of ion-surface collision spectra and table of total energies and heats of formation of species used in this study (6 pages). Ordering information is given on any current masthead page.

(57) Urquhart, G. G.; Gates, J. W., Jr.; Connor, R. *Organic Syntheses*; Wiley: New York, 1955; Collect. Vol. III, p 363.

(58) (a) Roothaan, C. C. J. *Rev. Mod. Phys.* **1951**, *23*, 69. (b) Binkley, J. S.; Pople, J. A.; Dobosh, P. A. *Mol. Phys.* **1974**, *28*, 1423.

(59) (a) Møller, C.; Plesset, M. S. *Phys. Rev.* **1934**, *46*, 618. (b) Carsky, P.; Hess, B. A., Jr.; Schaad, L. J. *J. Comput. Chem.* **1984**, *5*, 280.

(60) Binkley, J. S.; Pople, J. A.; Hehre, W. J. *J. Am. Chem. Soc.* **1980**, *102*, 939.

(61) Hehre, W. J.; Ditchfield, R.; Pople, J. A. *J. Chem. Phys.* **1972**, *56*, 2257.

(62) (a) Francl, M. M.; Pietro, W. J.; Hehre, W. J.; Binkley, J. S.; Gordon, M. J.; DeFrees, D. J.; Pople, J. A. *J. Chem. Phys.* **1982**, *77*, 3654. (b) Hariharan, P. C.; Pople, J. S. *Theor. Chim. Acta* **1973**, *28*, 213.

(63) Schmidt, M. W.; Baldridge, K. K.; Boatz, J. A.; Jensen, J. A.; Koseki, S.; Gordon, M. S.; Nguyen, K. A.; Windus, T. L.; Elbert, S. T. Program Package GAMESS. *QCPE Bull.* **1990**, *10*, 52.